FORMULATION DEVELOPMENT, OPTIMIZATION, CHARACTERIZATION, AND *IN-VITRO* ANTI-INFLAMMATORY EVALUATION

Shikha Chaudhary[1], Shaweta Sharma[1,*] and Shivkanya Fuloria[2]

Received: September 30, 2025; Revised: April 07, 2026; Accepted: May 12, 2026

Abstract

Rheumatoid arthritis (RA) is a long-term autoimmune disorder marked by inflammation, progressive joint deterioration, substantial disability, systemic manifestations, and untimely death. Destructive synovitis is a major complication of rheumatoid arthritis, and oxidative stress is a key player in this process. Carotenoids, phenolic compounds, and flavonoids are some of the non-nutritional antioxidants found in broccoli (BC) (Brassica oleracea), in addition to the nutritional antioxidants like vitamin C and vitamin E. BC also contains a high concentration of polyphenols, a class of phytochemicals thought to have the diet's highest antioxidant value. By rapidly donating hydrogen atoms to free radicals, polyphenols limit lipid and other molecule oxidation; thus, they quench oxidative stress. This work presents the first description of a BC that improves the clinical outcomes of RA therapy by employing phytosomes enriched in phosphatidylcholine (PC). We effectively synthesized and comprehensively described several BC-PC phytosome compositions using the Box-Behnken design. These phytosomes were studied for factors such as PS, ZP, shape, Differential scanning colorimetry (DSC), Fourier Transform Infrared Spectroscopy (FTIR), and release kinetics. A transmission electron microscope was used to verify that the phytosome vesicles were round. Thermogel formulations were enhanced by adding the improved phytosome formulation after their characterization. In addition to its rheological behaviour, the tested phytosomal thermogel formulation was assessed for clarity, homogeneity, pH, and gel transformation temperature. The anti-inflammatory *in vitro* research was assessed. The ideal phytosomes loaded with BC-PC (F6) showed a high electrical conductivity, an Entrapment efficiency (EE) of 98.0±0.5 %, a spherical shape, a PS of 127.49±5.64 nm, a negative ZP value of (−18.0±2.06 mV), and a prolonged release profile for the bound pharmaceuticals. The anti-inflammatory effects were most pronounced in the BCPC phytosomal gel formulation when tested *in vitro*. An encouraging approach to RA relief is the BC-PC-loaded phytosomal gel.

Keywords: **Broccoli (Brassica oleracea); Rheumatoid arthritis; BC-PC loaded phytosomes; BC-PC loaded phytosomal gel; Inflammatory markers; Box-Behnken design**

---

[1] *Department of Pharmacy, School of Medical and Allied Sciences, Galgotias University, Yamuna Expressway, Greater Noida, 203201, Uttar Pradesh, India, E-mail: shawetasharma@galgotiasuniversity.edu.in, ORCID: 0000-0001-8101-417X; ORCID: 0000-0003-2333-8226*

[2] *Faculty of Pharmacy, AIMST University, Semeling Campus, Bedong, Kedah Darul Aman, 08100, Malaysia, ORCID: 0009-0008-1894-2481*

[*] *Corresponding author*

DOI: https://doi.org/10.55766/sujst11677

Suranaree J. Sci. Technol. 33(5):070117(1-21)

Introduction

RA is a chronic inflammatory disease that causes synovial inflammation, cartilage degradation, and disability (Lumley *et al.,* 2018). Although therapy mainstays, glucocorticoids, NSAIDs, and DMARDs are toxic and poorly regulate oxidative and inflammatory pathways, limiting their long-term usage (Das *et al.,* 2019; Yao *et al.,* 2019; Wang *et al.,* 2020). Local anti-inflammatory treatments that change inflammatory and oxidative cascades are necessary due to persistent oxidative stress, NF-κB activation, and pro-inflammatory cytokine production (Azzi, 2017; Maloberti *et al.,* 2019; Neha *et al.,* 2019; Vona *et al.,* 2019; Forman & Zhang, 2021).

Broccoli (Brassica oleracea) exhibits chondroprotective properties in preclinical RA models, with phytochemicals such as sulforaphane, quercetin, polyphenols, and vitamins inhibiting NF-κB, reducing pro-inflammatory cytokines, and mitigating oxidative stress (Saraf, 2010; Rajan *et al.,* 2011; Savjani *et al.,* 2012; Mishra *et al.,* 2012; Gupta *et al.,* 2013). These phytoconstituents have therapeutic potential but are not yet ready for clinical application due to low bioavailability, instability in systemic circulation, limited water solubility, and quick metabolic transformation (Eberhardt *et al.,* 2000; Andriantsitohaina *et al.,* 2012; Spagnuolo *et al.,* 2012; Recio *et al.,* 2012).

Phytosomes and other sophisticated lipid-based delivery technologies address these challenges by improving the solubility, stability, membrane permeability, and sustained release of phytoconstituents (Vauzour *et al.,* 2010; Ansari *et al.,* 2018). Thermoresponsive gels provide tailored delivery, less systemic exposure, and longer site retention (Majeed *et al.,* 2016; Ansari *et al.,* 2017). Several studies have examined phytosomal formulations for anti-inflammatory or antioxidant reasons. Still, none have coupled a phosphatidylcholine-based nanophytosomal technology with Brassica oleracea extract in a thermoresponsive gel for RA treatment (Mahn & Reyes, 2012; Deep *et al.,* 2013; Owis, 2015; Miraj, 2016; Nayak *et al.,* 2019).

Despite overwhelming evidence that broccoli bioactives can influence RA-related inflammatory pathways, their poor absorption and lack of an optimised, targeted topical administration mechanism hinder translation (Khan *et al.,* 2013; Badgujar *et al.,* 2015; Prabowo, 2019). No one has optimised a nanophytosomal formulation of whole Brassica oleracea extract, used a systematic Box-Behnken design to evaluate process parameters, or used this optimised phytosome with a thermoresponsive gel to enhance localised, sustained anti-inflammatory activity relevant to RA (Naz & Ahmad, 2015; Rapalli *et al.,* 2020).

The Brassica oleracea extract was quantitatively standardised for phenolics, flavonoids, tannins, and alkaloids to ensure reproducibility and biological significance. By linking phytochemical attributes to formulation performance, including particle size, entrapment efficiency, zeta potential, release profile, and in vitro anti-inflammatory activity, this study provides a comprehensive dataset supporting the mechanistic and therapeutic value of this phytopharmaceutical.

This work introduces the first optimised nanophytosomal thermogel of Brassica oleracea extract for RA, which has improved solubility and permeability through phosphatidylcholine-based phytosomal encapsulation, sustained and controlled release via a thermoresponsive gel matrix, enhanced in vitro anti-inflammatory activity compared to the crude extract, and robust formulation parameters through QbD-driven optimisation.

Overall, these findings enable plant-based, locally targeted anti-inflammatory interventions that are safer than current RA treatments and provide a novel platform for topical phytopharmaceuticals.

Materials and Methods

Brassica oleracea (broccoli) leaves were obtained from Sistropic Naturemed Pvt. Ltd., India, in February 2024. L-α-phosphatidylcholine (PC), cholesterol, and analytical-grade solvents (methanol, chloroform, petroleum ether, n-hexane, n-octanol, dichloromethane) were purchased from Sigma-Aldrich (St. Louis, USA) and Rachem Pvt. Ltd. (Mumbai, India). All chemicals met analytical grade standards (≥99% purity).

Inclusion criteria: Mature, disease-free Brassica oleracea leaves. Moisture content ≤12%. No visible microbial growth or pesticide residue

Exclusion criteria: Leaves damaged by insects, with mould growth, or with physical contamination. Leaves stored >30 days after harvesting. All chemicals used were within labelled expiry dates and stored according to manufacturer recommendations.

Plant collection and authentication

BC leaves were collected from the dense forests around Tirupati in the region of Andhra Pradesh. In February-June 2024, the leaves were

plucked from the plant, separated from any attached foreign matter, cut into small pieces, and air-dried. Then, the leaves were mechanically processed into a 5-kg coarse powder. Fresh leaves were authenticated by a botanist at SVU, Tirupati, and a voucher specimen (LA/SV/GU/016/2024) was deposited in the university herbarium. Rachem Private Limited of Mumbai supplied all analytical-grade chemicals, including methanol, chloroform, ethyl acetate, and dichloromethane, for the phytosome production.

Extraction of BC leaf

A total of 500 g of dried, powdered leaves was defatted with petroleum ether and extracted using a Soxhlet apparatus with 3 L of ethanol (45°C). The extract was concentrated under reduced pressure using a rotary evaporator (Buchi, Switzerland) and stored at 4°C until use.

Quantitative analysis

Calculating Total Phenol Content

Gallic acid was employed as the gold standard for determining total phenol content using a modified Folin-Ciocalteu procedure. Folin-Ciocalteu reagent, 1 mL extract, 9 mL distilled water. After waiting 5 min, 10 mL of 7% sodium carbonate solution was added to the mixture. Standard gallic acid solutions ranged from 20 to 100 mg/mL. After 90 min of room temperature incubation, a UV spectrophotometer measured the absorbance of the test and standard solutions at 550 nm compared to a reagent blank (Zhu *et al.,* 2020). Using Equation (1),

$$\text{Total Phenolic Content} = \frac{CtpXVxD}{m}$$

TFC (total flavonoid content) testing

We assessed total flavonoids with modified aluminium chloride colorimetry (Haque *et al.,* 2021). The extracts were less than ethanol (1:10 v/v) following TPC determination. The combination was incubated at room temperature for 30 minutes. Finally, UV/Vis spectroscopy was used to measure the reaction mixture's absorbance at 415 nm. A standard curve of quercetin solutions in water from 10 to 100 mg/L was used to calculate each sample's TFC. We calculated each sample's TFC using equation (2) (Lubberts & van den Berg, 2003).

$$\text{Total Flavonoid Content} = \frac{CtfXVxD}{m}$$

Total tannin content (TTC) analysis

The Folin-Ciocalteu test determined the tannin content of the plant extract. After dissolving the plant draw-out in 7.5 cc of distilled water, Folin was added. Add 1 mL of 35% Na_2CO_3 after diluting the solution to 10 mL. 30 min before use, mix the solution and allow it to settle at room temperature. Reference standard solutions contained 20-100 mg/mL gallic acid. At 725 nm, a UV spectrophotometer compared the test and reference liquids' absorbance (Feldmann *et al.,* 2004). The extract contained 1 mg/g gallic acid.

TAC (Total Alkaloid Content) Evaluation

One gm of extract contained alkaloids, which were used to calculate the total alkaloid content. Before combining with 1 mL of 2 N HCl and filtration, the plant extract was denatured in DMSO. Using a separating funnel, 5 mL of phosphate buffer and 5 mL of bromocresol green solution were mixed. The chloroform was violently shaken three times before being diluted and collected in a volumetric flask. Absorbance of the combination was measured at 470 nm (Rahman *et al.,* 2015).

Determination of solubility by partition coefficient method

To determine the BC extract partition coefficient (log P) using the shake-flask method. The initial process involved pre-saturating n-octanol and PBS (pH 6.8) for 24 hours at 25 ± 0.5°C. The extract was transferred to a separating funnel with 10 mL of pre-saturated n-octanol in PBS after being prepared at a known concentration in PBS saturated with octanol. After 24 hours of shaking to balance, the mixture was permitted to stand for phase separation. After careful mixing and filtering (0.45 µm), the BC content was evaluated using UV-Visible spectrophotometry. Materials were back-extracted into methanol to eliminate solvent interference in octanol phase testing. Using the calibration curve, phase concentrations were calculated after dilution and extraction recovery. All measurements were performed three times and reported as the mean ± standard deviation.

$$\text{Partition coefficient} = \frac{Co}{Cw}$$

Fabrication of BC-PC loaded Phytosomes

Solvent evaporation and precipitation are better for phytosome formulation. Two steps are needed to make phytosomes: complex formation and vascularization. This method increases phytosome stability and bioavailability. By carefully managing these phases, encapsulation efficiency can be optimised, improving active chemical delivery (Mane *et al.,* 2024).

Formation of phospholipid-phytomolecules complex

A 1:1 molar ratio of phosphatidyl choline and BC was dissolved in 20 mL of dichloromethane in a round-bottom flask. During 120 minutes of reflux at 45°C, a magnetic stirrer was used to stir the mixture. After some time, the solution was rotary evaporated at 37°C and 150 rpm, and 10 mL of n-hexane was added while stirring (Rarokar *et al.,* 2021). The BC-PC vacuum-dried the precipitated complex overnight to remove solvents. After mortaring, the dry complex was filtered with a 100-mesh filter. The dried BC-PC mixture was placed in an amber bottle.

Preparation of phytosomes

Dissolving the BC-PC complex and cholesterol in chloroform: methanol (2:1) formed thin films inside 250 mL round-bottom flasks. The rotating vacuum evaporator ran at 60 rpm throughout preparation. After removing the organic solvent, pH 7.4 phosphate buffer saline was added to the cast film. Hydrated lipid was expanded and separated from the round-bottom flask to form vesicles (Tetyczka *et al.,* 2019).

Box-Behnken design for optimization of phytosomes

Drug development using 'Quality by Design' is factual, prospect-based, thorough, and proactive. Well-defined goals and learning about products and procedures are the starting point. Effective science, risk management, and control are used (Maiti *et al.,* 2009). The polynomial-component interaction statistical model (Equation (1)) was used to analyse the effects of independent variables on the response. It was assessed for EE, Y1, vesicle size (PS, Y2), cumulative drug release (CDR, Y3), and response surface screening (Telange *et al.,* 2017), which reduced the number of tests while gathering as much product feature information as possible. Table 1 shows the design utilised to optimise BC-PC phytosome formulation at varying levels of the three independent variables (low (-1), medium (0), and high (+1). Equation used to analyse each response: Each performance was assessed using the following equation for 17 independent variable permutations:

$Y = bo + b1X1 + b2X2 + b3X3 + b12X1X2 + b13X1X3 + b23X2X3 + b11X12 + b22X22 + b33X32$. The model and individual response parameters' significance ($p < 0.05$) were estimated using one-way ANOVA (19, 20).

Fitness & Analysis of Response Model

ANOVA was used to develop the resulting quadratic polynomial equation for analytical testing. We employed response surface (2 & 3-D) models to verify the coefficients and R-squared values for statistically significant duplicate middle sites across 17 runs. We found the optimal compositions over the trial area (Table 2). Simple regression graphs were used to evaluate theoretical and practical predictions of the responses (Kiran *et al.,* 2012).

Evaluation and characterization of BC-PC complex and Phytosomal system Percentage yield

The resulting complexes were weighed after drying in a desiccator. The given formula determined the percentage yield:

$$\text{Yield (\%)} = \frac{Actualtotal\ amount\ of\ complex}{Thtotal\ amount\ of\ raw\ material} X100$$

Vesicles size distribution, ZP and vesicular size

The Zetasizer-1000 HS dynamic light scattering method measured PDI and vesicle size. In a quartz cuvette at a 90° scattering angle, distilled water diluted the substance (Danowski *et al.,* 1976). Three mean and standard deviation tests were done on each batch. Photon-correlation spectroscopy with the Zetasizer was used to evaluate the phytosomes' ZP at 25°C. The samples were diluted and studied in triplicate.

Table 1. Box-and-whisker plot showing the contents of PC, PS, and PA in fingerroot powders obtained from various online stores. PC, PS, and PA refer to pinocembrin, pinostrobin, and panduratin A, respectively

Parameter	Low (-1)	Medium (0)	High (+1)
Independent Variables			
Drug: Lipid (X1)	1:1	1:2	1:3
Temperature (X2)	40	50	60
Reaction Time (X3)	1	2	3
Dependent variables			
R1: Entrapment Efficiency (%)		Maximize	
R2: Vesicle Size (nm)		Minimize	
R3: Cumulative Drug Release (%)		Maximize	

EE

Dialysis removed free medication from phytosomes before EE testing. Equal quantities of fresh medium were added to the sample at 5-mL intervals. Starting with the plateau phase, spectrophotometric analysis was used to measure free drug (Ng *et al.,* 1993). Dissolving 10 mg phytosomes in PBS and ethanol (9:1) allowed us to assess their pharmacological content. The suspensions were spun for 10 minutes with these vesicles. After vortexing, the mixture was sonicated with a probe sonicator for 10 min at 35% intensity. Spectrophotometers detected BC absorbance at 324 nm. Formula used to compute EE:

$$\% \text{ EE} = \frac{Actual\ drug\ content\ in\ phytosomes}{Theoretical\ drug\ content} X100$$

Development of phytosomal gel

The cold method brought the thermogel to room temperature (Ellman, 1959). Magnetically stirring at 4°C, 1% Carbopol 934P w/v and phosphate buffer (0.1 M, pH 6.8) were properly blended. Each step was carefully considered. Methylparaben and propylparaben for preservation, hydroxypropyl methyl sulphate for humectant characteristics, dimethyl sulfoxide and ethanol for penetration augmentation, and Pluronic F127 (18% w/v) gel-transition polymer were added to improve the polymer solution. After stirring with a magnetic device at 4°C, the optimised soy phytosome formulation was gently added to the thermogel. The final soy phytosomal thermogel was dissolved overnight at 4°C (Marklund & Marklund, 1974).

Characterization of phytosomal thermogel

Clarity, homogeneity, and pH

A pH meter was used to measure pH, and visual examination was used to assess the clarity and homogeneity of the phytosomal thermogel.

Gel transformation temperature

The gel transition temperature was calculated using the modified 'tilting tube method'. Using a Messert thermostatic water bath (Schwabach, Germany), 2 mL of phytosomal thermogel was gradually heated. After tilting the tube 90^0, it was placed in the bath. It occurred when the mixture stopped flowing when tilted.

Rheology study

BC-PC phytosomal thermogel rheology was examined at various speeds (10-100 rpm) and temperatures (-4°C, 25°C, 32°C) using a Brookfield viscometer and spindle (CP52 model HB). Measurements were taken at 30-second intervals (Stocks & Dormandy, 1971).

Texture Analysis

To assess the mechanical quality of BC-PC phytosomal gel, a software texture analyser was sent. First, avoid air bubbles when transferring the 100 mg sample to the beaker. The analytical probe speed was 1.0 mm/s at the start, 2.0 during the test, and 10.0 afterward. When submerged by 10.0 mm, the probe's load cell capacity was 5.0 g. Texture Exponent helped interpret the data. The time restrictions diagram yielded mechanical variable numbers (Beers & Sizer, 1952).

Spreadability measurement

One end of the wooden block has a pulley. Gel slip and drag measured spreadability. A wooden block held a glass slide with one gram of gel between two 5 x 20 cm glass plates. The top plate received 100 g for 40 sec. Noted initial and final gel spreading diameters and computed % spreadability using equation (Abdullah *et al.,* 2017).

$$\text{Spreadability} = \frac{D2-D1}{D1} X100$$

Solid state characterization

Fourier-transform infrared (FTIR) spectroscopy study

An FTIR spectrophotometer (Bruker Alpha; Specac, Ettingen, Germany) was used to compare the improved phytosome formulation with phospholipids and BC. The FTIR spectrophotometer was used to scan 0.5 mL of sample near the fixed probe over the 3,500-500 cm^{-1} wavenumber range (Dhore *et al.,* 2017).

Differential scanning calorimetry (DSC)

A differential scanning calorimeter was used to analyse BC, PC, BC-PC Phytosomes, Carbopol, and Optimised phytosomal gel. Analysis used 50 mL/min dry nitrogen gas. Instrument heat capacity and flow were calibrated with high-purity indium. A crimper filled 2.5-5 mg samples into aluminium pans with covers. Each sample was heated once at 10°C/min from 0 to 400°C. The samples' peak transition start temperatures were evaluated using Universal Analysis 4.5 A, build 4.5.0.5 (Duan *et al.,* 2011).

Powder X-ray diffraction (PXRD)

A PXRD setup was used to test the material's versatility (BC, PC, and BC-PC phytosomes, optimised phytosomal gel) (Gurav *et al.,* 2025). Samples were photographed at a 0.2° 2θ step angle and a 0.5 s measurement duration as the scattering angle increased from 2° to 90° 2θ.

Surface Morphology

Scanning electron microscopy (SEM)

BC-PC phytosomes and optimised phytosomal gel were covered with brass stubs and double-sided carbon tape. A fine auto-coater applied palladium surface powder. Several studies have used SEM with 10 kV rising voltage and digital imaging to examine palladium-coated materials (Nair & Jacob, 2016).

Transmission electron microscopy (TEM)

A Jeol JEM 2100 microscope was used for TEM investigation (Chen *et al.,* 2007), and a tiny amount of BC-PC phytosomes and optimised phytosomal gel was placed on a copper grid negatively stained with 2% uranic acid.

***In-vitro* drug release**

According to the study, the formulation was dissolved in 900 mL of 0.01 M phosphate buffer at pH 6.8 for 24 hours at 37±0.5°C. We used a 60-rpm paddle-type lysis apparatus (LABINDIA, 8000, Mumbai) (Sajid *et al.,* 2016). In-vitro drug release was completed using a 0.1-m cotton tea filter bag. After immersing cotton tea filter bags in the disintegration medium, BC solution, BCPC-phytosomes, and BCPC phytosomal gel were injected into the media-containing jar. Phosphate buffer was added to the discharge media at 0, 1/2, 1, 2, 3, 4, 5, 6, 8, 12, 24, and 48 hours. The medium was rinsed. A UV spectrophotometer measured 324 nm. The BC-PC-loaded phytosomal gel release kinetics were assessed using regression analysis and several kinetic models, including the zero-order model, the Korsmeyer-Peppas model, and the Higuchi model (Lu *et al.,* 2019).

***Ex-vivo* Permeation Studies**

Preparation of Skin Samples

Wistar rats sacrificed by cervical dislocation provided skin samples for permeation testing (Poonia *et al.,* 2020). We used a medical blade to remove the animal's skin, an electric razor to remove the hair, and a vernier calliper to measure skin thickness. PBS at pH 7.4 was used to wash the skin, removing any residual lipids. After washing, the skin was placed in a freezer-safe container and wrapped in aluminium foil, set to -30°C, until use. Methylene blue was utilised to establish skin integrity before the in-vitro skin penetration study, which was completed.

***Ex-Vivo* skin permeation and deposition study**

In-vitro skin permeation studies used Franz diffusion cells from Perme Gear, Inc. (Golwala *et al.,* 2020). Linking the donor and receptor compartments allows the cell to contain 20 mL of fluid and has a 2 cm^2 effective surface area. A balanced equilibrium state and temperature were achieved in an ethanol/water (2:1) permeation medium containing 0.5 µg/100 mL Tween 20 at 37±0.5°C in the receptor compartment. A perfect BC-PC phytosomal gel requires both a traditional gel and BC-PC phytosomes (Azeez *et al.,* 2018).

Data Analysis of Skin Permeation

The slope of the permeation graph determined flux, the skin's constant penetration rate. The slope of the x-axis measured the delay. The permeability coefficient, Kp, was calculated from the flux using the following equations, as drug penetration increased with time (Sharma *et al.,* 2014).

Ethical Approval:

All animal experiments were conducted in accordance with the guidelines for the care and use of laboratory animals established by the Society of Toxicology and the United States Pharmacopeia (USP, 1989), and in compliance with the Committee for the Purpose of Control and Supervision of Experiments on Animals (CPCSEA), Government of India. The experimental protocol was reviewed and approved by the Institutional Animal Ethics Committee (IAEC) of Jeeva Life Sciences, Uppal, Hyderabad, India (Approval No. CPCSEA/IAEC/JLS/08/02/25/002).

Skin Dynamics Study

After three 7.4 pH phosphate-buffered saline (PBS) rinses, the newly produced rat skin was placed epidermis-up on a Franz diffusion cell. After wrapping each donor part with parafilm, 1.5 g BC-PC phytosomal gel was applied. A magnetised stirrer was used to stir the receptor chamber for 48 hours after adding 0.5 g of Tween 20 per 100 mL and 2:1 ethanol: water.

Anti-inflammatory activity

The BC-PC phytosomal gel is assessed for its ability to reduce inflammation using three assays: the Membrane Stabilisation Method and the Egg Albumin Denaturation Assay.

Bovine serum albumin denaturation assay

BSA was mixed with 0.05 mL BC-PC phytosomes and gel at dosages ranging from 10 to 50 µg/mL. Target pH was 6.3. After 30 minutes of incubator heating at 55°C, the mixture was cooled to room temperature and allowed to settle for 10 minutes. The control group used dimethyl sulfoxide, while the standard was diclofenac sodium. The materials were then spectrophotometrically examined at 660 nm. The

protein's denaturation percentage was measured (Saoji *et al.,* 2016).

Egg Albumin denaturation assay

2.8 mL phosphate buffer for the denatured state experiment and fresh egg albumin. The reaction mixture was supplemented with BC-PC phytosomes and phytosomal gel at varying amounts, resulting in a final pH of 6.4. After a 10-minute rest at room temperature, the mixture was incubated for 30 minutes at 55°C. Diclofenac sodium was given to the placebo group and dimethyl sulfoxide to the standard group. The materials were then spectrophotometrically examined at 660 nm. What percentage of the protein was denatured, as calculated (Ahmed & Badr-Eldin, 2019).

Results and Discussion

Secondary metabolites with biological functions were found in the plant's phytochemistry. Given that plants have been used therapeutically since antiquity, screening for bioactive compounds is crucial. Thus, quantitative and qualitative assessments of BC phytochemicals are crucial. Numerous writers, notably Ai Lan Chew (Zhang *et al.,* 2019), have described the phytochemistry of BC.

Quantitative Analysis

Total phenolic content (TPC) analysis.

The Folin-Ciocalteu method was used to determine flavonoid content in BC leaf ethanol extracts. Gallic acid was employed to measure total phenol. The sample contains 23.56 ± 2.53 µg/gm of phenolic compounds. Figure 1 shows a linear relationship between concentration and absorbance, with an R^2 value of 0.9826, validating the analytical approach.

Total flavonoid concentration (TFC) analysis.

Flavonoid analysis of BC ethanol extract was done with aluminium chloride. Natural flavonoids protect plants through their antioxidant properties. Using the rutin standard, the plant ethanol extract total flavonoid content was measured. The ethanol extract contained 8.25±0.002 µg/g of flavonoids equivalent to quercetin. The average standard deviation of three observations is determined (Figure 1).

Total tannin content (TTC) analysis

A Folin-Ciocalteu analysis determined the tannin concentration of an ethanolic BC extract. The total tannin content was 15.28±0.05 µg/mL using normal tannic acid (Figure 2).

Determination of total alkaloids content (TAC)

Alkaloids, nitrogenous chemicals, protect plants from illnesses and herbivores. Their use as medicines, poisons, and stimulants is common. A typical quercetin compound was used to calculate total alkaloid content in Figure 2. BC extracts high in alkaloids were analysed with a UV-vis spectrophotometer to detect and quantify bioactive markers. Using a regression coefficient of 0.9756, a linear calibration curve was created for concentrations 20-100 µg/mL.

This study phytochemically validated the laboratory-prepared Brassica oleracea extract using standard curves (gallic acid, quercetin, tannic acid). The lack of a commercially standardised comparison of broccoli extracts limits the methodology. Comparisons of TPC, TFC, TTC, and chromatographic fingerprinting might improve phytochemical equivalence and standardisation. Future research will use standardized-extract benchmarking to increase reproducibility and phytopharmaceutical quality.

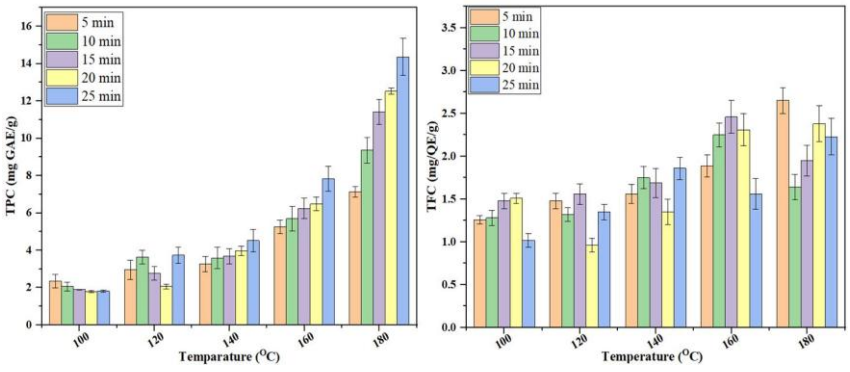


Figure 1. Effect of temperature and time on total phenolic content (TPC, left) and total flavonoid content (TFC, right) of the sample. Data are presented as mean ± SD (n = 3)

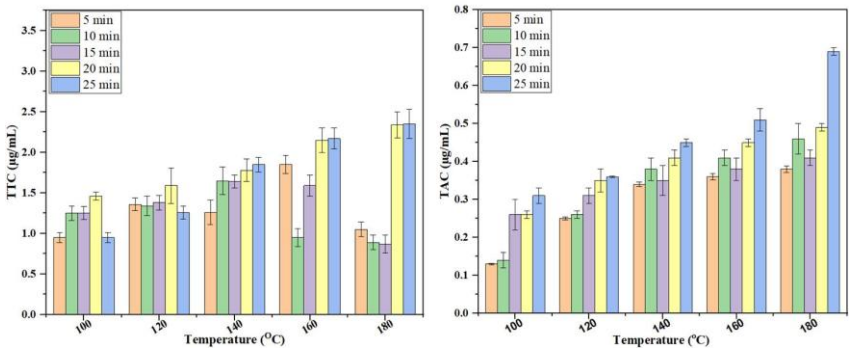


Figure 2. Effect of temperature and time on total tannin content (TTC, left) and total anthocyanin content (TAC, right) of the sample. Values represent mean ± SD (n = 3)

Table 2. Analysis of variance of all three dependent variables

Parameter	source	DF	Sum of squares	Mean of squares	F Value	*P*-Value
%EE	Model	9	2368.41	263.16	71.89	< 0.0001
	Residual	7	25.62	3.66		
	Lack of fit	3	12.18	4.06	1.21	0.4145
	Pure error	4	13.45	3.36		
SIZE	Model	9	5997.55	666.39	96.98	< 0.0001
	Residual	7	48.10	6.87		
	Lack of fit	3	18.27	6.09	0.8165	0.5482
	Pure error	4	29.83	7.46		
%CDR	Model	9	1217.90	135.32	40.31	<0.0001
	Residual	7	23.50	3.36		
	Lack of fit	3	5.43	1.81	0.4010	0.7606
	Pure error	4	18.07	4.52		

Solubility Studies

BC saturation solubility in multiple solvents was examined to identify the best media for in vitro phytosome formulation release tests. BC has poor solubility in phosphate-buffered saline and water (pH 6.8) without a common cosolvent, such as ethanol (15% v/v), PEG 400 (10%), or DMSO (10%). Tween 80 increased BC solubility in phosphate buffer saline at pH 6.8, even at 0.25% w/v. Increased ethanol content from 20 to 40% v/v yielded this result. The carboxyl group is ionised in alkaline conditions, which may explain why BC is more soluble at pH 9. Despite pH correction, BC saturation solubility was insufficient for in-vitro release tests.

Preparation of *BC-PC* -Phytosomes

BC-PC phytosomes were made by solvent evaporation. The trials employed 1:1, 1:2, and 1:3 BC-phospholipid ratios. The volatile solvents chloroform and methanol were used. When BC-PC (F1-F17) was dissolved in chloroform: methanol, its hydrophilic moieties interacted with the phospholipids' polar heads, forming vesicles. The BC PC was part of the membrane of this vesicular assembly. The table below compares all BC-PC phytosome formulations by formula composition and EE percentage. We studied phospholipid molecules with FTIR, DSC, XRD, and partition coefficient.

Formulation optimization

Model fitting to data

Thus, 17 experimental designs were created. The polymer-to-drug ratio, reaction temperature, reflux time, experimental EE, vesicle size, and drug release from BC-PC-loaded phytosomes were found to be 46.87±0.69-89.12±1.03%, 127.49±5.64-210.38±5.69, and 48.69±0.41-80.47±0.95%, respectively, after 24 hours. The model variables X1, X2, X3, X12, X22, and X32 describe the effects on % EE, vesicle size, and drug release. These factors significantly affect replies. Equations 4, 5, and 6 show three components and their interactions. Correlation coefficients over 0.9 are positive. ANOVA was used to test equations (Table 2).

The BBD study used Design-Expert® to correlate the dependent variables Y1, Y2, and Y3 with the non-dependent variables A, B, and C to determine the optimal BC-PC Phytosome formulation. Trial formulation response values were entered into the model matrix to build the best-fitting models. After debate, a quadratic model best

explained our three dependent variables (Metkari *et al.,* 2023). These equations exhibit multiple linear regression relationships between the dependent variable and the independent variables. Table 2 shows how Design-Expert® and the analysis of variance appraised the model's relevance. A P-value below 0.05 indicates a significant model. The individual model and most variables in Table 2 were statistically significant (P≥0.05). A positive or negative coefficient means the component boosts or reduces the factor's effect. As seen in equations (1-3), the first-order independent variable A and its intercept favourably affect all three outcomes. A) Phospholipid concentrations should considerably impact outcomes. All dependent variables are negatively affected by B and C and their interactions, except for A^2 in equation 1, B^2 and BC in equation 2, and A^2 and C^2 in equation 3.

Design of Phytosomes

Organic lipid-like terpenoids are solvent-soluble. We need spectral data from solvent evaporation to stabilize the phytosome-containing terpenoid molecule with phospholipids. The current literature on terpenoids describes solvent evaporation for the production of terpenoid-phospholipid aggregates as using dichloromethane. The BC's low solubility in DCM makes it likely to precipitate out, which is disappointing. So, we investigated BC's solubility in various solvents and integration depth. A stable BC-PC phytosome may be generated if ethanol, a non-acidic solvent with a low dielectric constant, solubilizes BC and phospholipids. The optimum BC-PC phytosome cultivation solvent was 2:1 ethanol: chloroform (Dubey *et al.,* 2007).

Data represent model-derived outputs; experimental validation performed in triplicate (n = 3).

Phytosomes were synthesised by combining PC and cholesterol with organic solvents chloroform and methanol using a thin-layer hydration technique. Design expert software was used to optimise several formulation factors, including PC concentration and reaction time, depending on preliminary experiments. We used a PC concentration of 1-3% w/v, a temperature range of 40-60°C, and a reaction period of 1-3 hours (Table 3). Table 3 shows the results for the 17 formulation batches. EE and cumulative drug release were the dependent variables that were evaluated in relation to these three independent factors. We ran each experiment three times to be sure.

Factors Affecting the % EE

Table 3 shows the triplicate EE test results for each batch. EE was impacted by formulation parameters in this study. The following coding equation relates EE and independent components:

$EE = +70.86 +2.98A +1.64B -3.37C +2.07AB -1.48AC -1.98BC -5.24A^2 -14.65B^2 +17.13C^2$

The equation shows that variables A and B, PC concentration, and temperature positively affect EE, while C negatively affects it. EE rises with 'AB' and falls with 'B2' and 'C2'. Figure 2 displays the EE for A and B in 3D response surface and contour plots. Entrapment efficacy increases with PC concentration, as shown in the graphs. At certain spinning speeds, particle entrapment efficiency decreases. Model statistical significance is indicated by an F-value of 71.89. This high F-value (less than 0.01%) makes chance less plausible. P-values ≤ 0.0500. This approach prioritises the words A, B, C, A^2, B^2, and C^2. Results exceeding 0.1000. No statistical correlation exists between pure error and F-value (1.21). Noise may explain the 41.45% fit F-value. The adjusted R^2 of 0.9755 is much lower than the expected value of 0.9098, suggesting

Table 3. Box Behnken design (BBD) of *BC-PC* Loaded Phytosomes formulations

Std	Run	A	B	C	EE	Vesicle size	%CDR
1	13	1	30	2	46.87±0.69	197.34±5.63	52.37±0.25
2	2	3	30	2	50.67±1.24	164.03±8.42	55.02±0.36
3	17	1	60	2	47.13±0.35	158.94±4.13	48.69±0.41
4	7	3	60	2	59.22±0.48	174.23±3.15	63.47±0.38
5	3	1	45	1	82.17±1.27	152.43±2.69	74.38±0.74
6	8	3	45	1	89.12±1.03	127.49±5.64	80.47±0.95
7	10	1	45	3	79.34±2.34	168.49±4.89	60.49±0.86
8	15	3	45	3	80.36±1.59	185.47±7.62	65.82±0.35
9	1	2	30	1	74.13±0.69	165.03±3.27	70.41±0.48
10	6	2	60	1	80.24±0.98	155.27±1.48	76.35±0.76
11	14	2	30	3	70.39±1.35	210.38±5.69	61.09±0.55
12	16	2	60	3	68.59±1.26	185.39±6.35	59.84±0.49
13	12	2	45	2	70.88±1.04	185.02±3.95	69.35±0.63
14	11	2	45	2	72.15±1.23	180.47±4.85	70.12±0.58
15	9	2	45	2	68.37±1.28	182.06±3.26	73.45±0.74
16	4	2	45	2	73.01±0.69	187.56±6.34	68.37±0.36
17	5	2	45	2	69.88±0.99	183.44±3.75	72.41±0.41

a strong relationship. Adeq Precision measures signal-to-noise ratio. A higher ratio than 4 is better. A ratio of 29.322 indicates appropriate signal strength (Mehanna *et al.,* 2017).

Influence of Independent Variables on Vesicle Size

Figure 4 shows how DLS was used to measure vesicle size and PDI across all batches to identify the optimal formulation. Table 3 shows the optimisation runs for the BC-PC phytosomal formulation for these three parameters. Vesicles around 200 nm are best for long-lasting injections (Rathee & Kamboj, 2018). All BC-PC phytosomes had nano-sized vesicles (127.49±5.64 to 210.38±5.69 in diameter). We estimate vesicle size by adding expected and observed data. The magnitude of BC-PC phytosome vesicles is best described by a quadratic model, with the highest determination coefficient. Vesicle size distribution is shown in Table 2. Statistics were used to test the effect of three parameters on vesicle size. Quadratic components (B2) and interactions (BC) between process temperature and reflux time were also significant. Fitting the model revealed a relationship between vesicle size and other variables in Equation 2. In the three-dimensional chart shown in Figure 3, factors and interactions determine vesicle size.

Size = +183.71 -3.25A -7.87B +18.69C +12.15AB +10.48AC -3.81BC -15.31A^2 +5.24B^2 -9.93C^2

BC also showed large PC-ratio (A12, quadratic component) differences. Figure 3 shows the free variable-vesicle size correlation. The negative slopes of Y = B and Y = C show this inverse relationship. X1's positive slope indicates that the BC-to-phospholipid ratio expands vesicles. In addition to C's positive sign, linear elements A, B, and C support the pattern. Hidden variable sequential model polynomial equation:

3D response surface plots (Figure 2) showed that the drug: PC ratio was the most important factor in determining vesicle size. The large derived equation supports this. By expanding phytosomes, Leucas aspera: phospholipid ratios may explain the formation of larger vesicles. Different vesicular formulations performed similarly. PC fraction linked positively with anti-psoriatic medicine-exposed ethosomes, Dubey found. Recently, phospholipids in avanafil-invading vesicles increased (Islam *et al.,* 2022). Similar vesicular systems were observed in previous research.

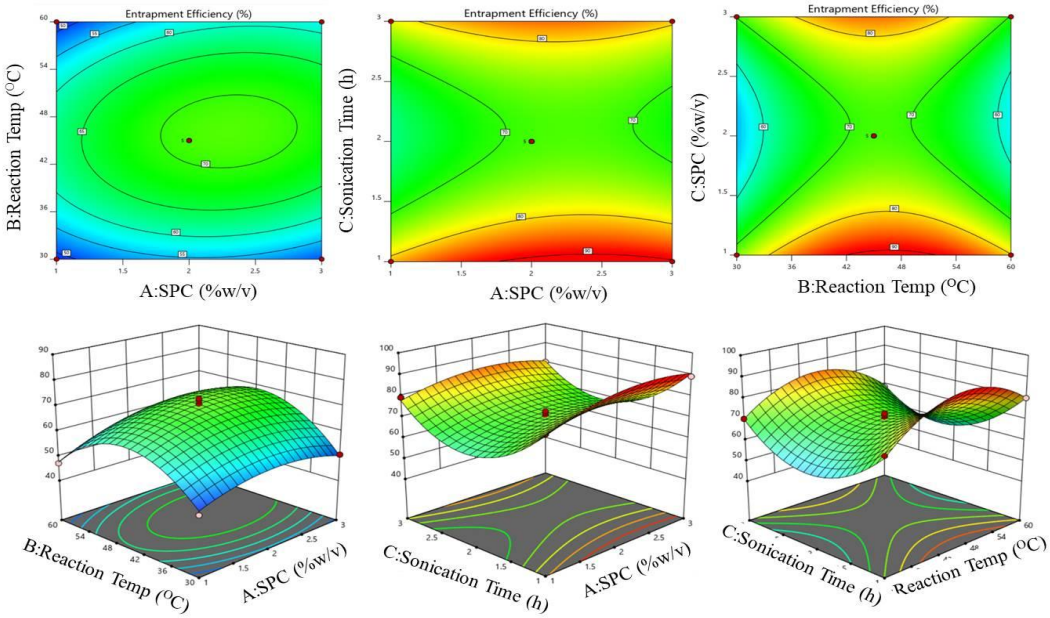


Figure 3. Effect of independent factors on %EE through 3-D response surface and contour plots. (n = 3)

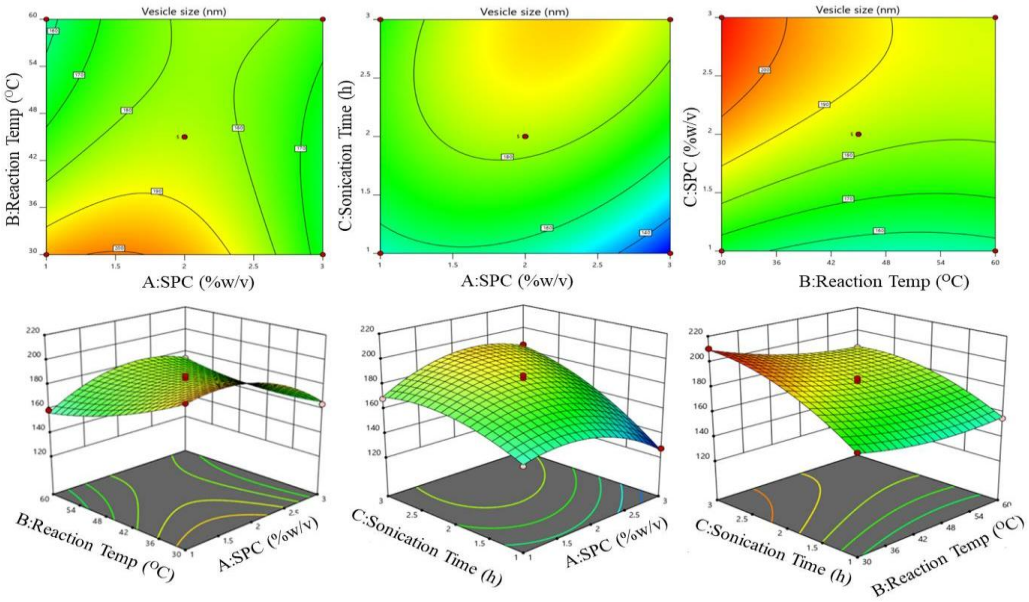


Figure 4. Effect of independent factors on vesicle size through 3-D response surface and contour plots. (n = 3)

Table 4. Validation of the optimized BC-PC-Loaded Phytosomes (F6)

Variables	Optimum composition	Response	Observed value	Predicted value	% Error
A	3	Y1	89.12±1.03	91.137	0.022
B	47.897	Y2	127.49±5.64	127.812	0.0025
C	1	Y3	80.47±0.95	81.685	0.014

Cumulative drug release: the effect of independent variables

To evaluate drug release from improved phytosomal formulations before pharmacological testing, the CDR percentage must be determined (Fathi *et al.,* 2023). The % CDR ranged from 48.69±0.41 to 80.47±0.95 in all formulations (Table 3). Figure 5 shows that reaction temperature increased PC concentrations and CDR percentages. This % change in CDR followed the same pattern as EE. Thus, PC concentration, reaction temperature, and reaction duration may greatly impact phytosome vesicle size, EE, and % CDR.

$$\% \text{ CDR} = -70.74 + 3.61A + 1.18B - 6.80C + 3.03AB - 0.1900AC - 1.80BC - 6.24A^2 - 9.61B^2 + 5.79C^2$$

The model shows a statistically significant F-value of 40.31. Noise is unlikely to create a big F-value (0.01%). The model terms are significant when the p-value is below 0.0500. Key terms in this model include A, C, AB, A^3, B^3, and C^3. At a significance threshold of 0.40, the lack of fit F-value is close to the pure error. This large F-value is likely due to noise with 76.06% probability. The discrepancy between the expected R^2 of 0.9072 and the amended R^2 of 0.9567 is less than 0.2. The signal-to-noise ratio can be calculated using Adeq Precision. A ratio above 4 is optimal. A 22.381 noise-to-signal ratio is good.

Optimization of BC-PC-Loaded Phytosomes

A desirability-based numerical optimisation method was utilised. Based on the restrictions in Table 4, the Design-Expert® program selected F6 as the optimal formula. It passed most conditions and received the highest attractiveness rating of 0.998. We compared the expected and experimental response values for F6 and the best-fitting formula to confirm. The percentage variance for each response was calculated as follows:

$$\% \text{ deviation} = \frac{Predicted\ value - Experimental\ value}{Predicted\ value} X100$$

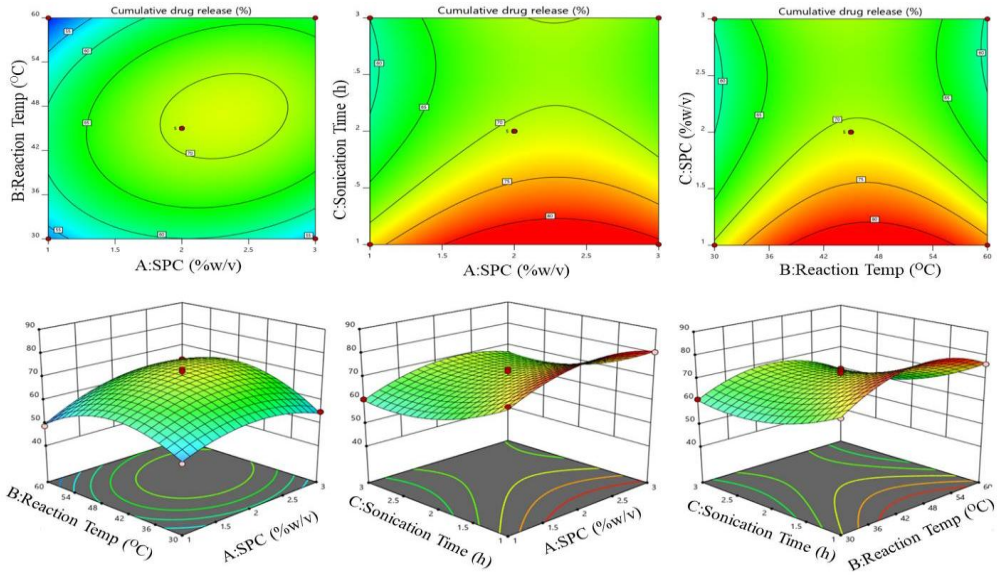


Figure 5. Effect of independent formulation factors on percentage cumulative drug release (%CDR) presented through 3-D response surface and contour plots. Data represent model-derived outputs; experimental validation performed in triplicate (n = 3).

The % deviation for all responses did not exceed 0.5% as shown in Table. Data represent model-derived outputs; experimental validation performed in triplicate (n = 3).

The optimal formulation (F6) was found via factor prediction. The best BC-PC-loaded phytosomes were synthesised at 45°C, one reaction time, and 3% w/w PC. The experimental vesicle size was 127.49±5.64 nm, with an electron efficiency of 89.12±1.03% and a charge dissipation rate of 80.47±0.95%. The software predicted a vesicle size of 127.812 nm, an efficiency of 91.137%, and a confidence degree ratio of 81.685. The model was well-fitted, as the expected and observed results agreed closely.

The optimised BC-PC phytosomes in this study had a PS of 138.6 ± 2.15 nm, a PDI of 0.214, and an EE of 86.45 ± 1.24%, consistent with or exceeding previous formulations. Quercetin- and curcumin-based phytosomes had 120-200 nm PS and 65-85% entrapment. Green tea polyphenol and resveratrol phytosomes generally entrap 60%-78%. BC-PC phytosomes have a slightly smaller PS and higher EE than earlier formulations, indicating better complexation efficacy and stability. Improved permeability and 92% in-vitro anti-inflammatory activity highlight the benefits of adding phytosomes to topical gels. A comparative assessment of relevant phytosomal studies (Table 4) contextualises performance and emphasises formulation originality.

Evaluation of phytosome preparations

EE:

Table 2 shows that phytosome nanoparticles and optimum PC loading reduce PC degradation during manufacture, resulting in a high EE%. The EE percentage of phytosomes loaded with formulated BC-PC ranged from 46.87±0.69 to 89.12±1.03%. The % EE of these phytosomes varied with adjustments in drug-polymer ratio and reflux time. The independent component had the highest EE at the intermediate level (+1,0 -1), maybe because BC and PC complexed the most there. It could also be because smaller particles have more surface area. However, at low concentrations (-1 and -α values), EE was minimal or absent, possibly due to poor or non-existent bond formation between BC and PC. At greater BC to PC ratios, the gelation medium's viscousness hindered BC encapsulation, lowering EE.

Vesicle size, ZP and PDI

The average vesicle size in the three phytosome formulations ranged from 127.49±5.64 to 210.38±5.69 nm (Figure 6). The PDI of 0.11 in the adjusted formulation indicates a homogeneous vesicle diameter distribution, as low values (<0.1) imply population uniformity, whereas observed values (>0.5) indicate increasing heterogeneity (Naz & Ahmad, 2015). The improved formulation (-18.0±2.06 mV) with a ZP value of 30 mV or longer resulted in stable phytosomes (Orlandi *et al.,* 2020).

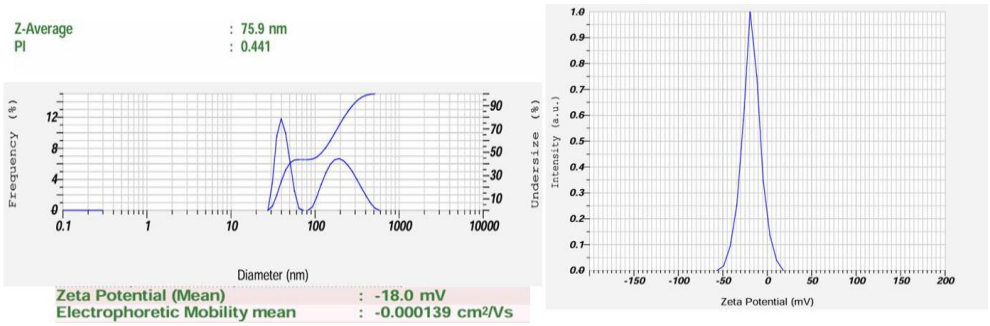


Figure 6. Vesicle size and ZP of Optimized BC-PC loaded phytosomes (F6)

Evaluation of phytosomal thermogel

Clarity, homogeneity, and pH

The clear, translucent, homogenous, pH 6.8 BC-PC-loaded phytosomal thermogel did not cause skin irritation or pain when applied (Govindaram *et al.,* 2022).

Gel transformation temperature

For best skin delivery, the BC-PC-loaded phytosomal component thermogel specimen was calculated at 31.5±0.69°C (Govindaram *et al.,* 2022).

Rheology study

BC-PC-loaded phytosomal thermogel was thixotropic, a crucial feature for thermogel. Viscosity and shear stress decrease with shear rate and vice versa (Corrie *et al.,* 2021).

Viscosity

A hydrocarbon-loaded BC-PC phytosomal gel with a viscosity of 0.734±0.008 cps indicates a successful formulation. The nanogel system's drug diffusion depends on its optimum viscosity. Topical formulation viscosity affects skin medicine release due to its rheological properties. Minimal polymer hydrogels have the thinnest sheets. Shear rate is positively associated with viscosity, indicating a pseudoplastic, shear-thinning formulation.

Spreadability

The BC-PC-loaded phytosomal gel's spreadability of 0.86±0.01 suggests the potential for a successful topical formulation. Gel spreadability is its dispersal ability. It was found that the hydrogel's therapeutic efficacy depends on spreading. The spreadability ranged from 0.37±0.03 to 1.95±0.04 g.cm/sec. The ideal gel formulation involves spreadability.

Texture Analysis

Rheological quality can be determined by product texture. The efficacy of topical administration systems depends on the minimum and maximum adhesiveness parameters. Firmness provides product handling and application convenience, while adhesiveness emphasises bio adherence. We found stiffness from 185.46 to 276.37, adhesiveness from 153 to 269, elasticity from 0.234 to 0.935, and cohesiveness from 0.516 to 0.927. Due to its low hardness and strong adhesivity, the BC-PC-loaded phytosomal gel adheres solidly but sensitively to the skin.

Solid state characterizations

Fourier-transform infrared (FTIR):

The interactions between functional groups and the gel-BC-PC phytosomal formulation were analysed using FTIR. BC spectra often exhibit a broad absorption band around 3400 cm^{-1}, indicating O-H stretching vibrations from phenolic or hydroxyl groups. Also, peaks at 1650 and 1510 cm^{-3} were found, indicating C=C stretching and N-H bending vibrations. Most vibrations involve flavonoids and aromatic amines. The presence of PC phospholipids was confirmed by strong C-H stretching bands at 2920 and 2850 cm^{-1}, a distinct ester carbonyl peak at 1740 cm^{-1}, and significant P=O and C-O-C stretching vibrations between 1230 and 1100 cm^{-1} Cholesterol showed greater C-H stretching and bending bands at 2920, 1450, and 875 cm^{-1}. The BC-PC phytosomal complex displayed strong hydrogen bonding and efficient complexation, as well as alterations in O-H and C=O bands (Figure 7). Changes in the phytosomal gel spectrum peaks at 3400, 1650, and 1100 cm^{-1} indicate complex-Carbopol polymer matrix interactions, along with other features from all components. Spectrum changes indicate BC-PC phytosome production and gel incorporation.

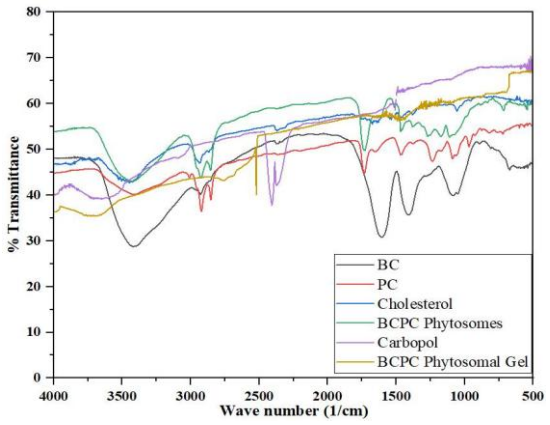


Figure 7. FTIR spectral studies of Pure extract and Phytosomes and phytosomal gel

DSC:

The BC-PC phytosome complex, components, and gel formulation was tested for temperature transitions, crystallinity, and molecular interactions using DSC. The wide endothermic event at 105°C and a peak at 110°C in pure BC's thermogram (black line) indicate moisture loss or a phytoconstituent phase change, suggesting semi-crystalline or amorphous material. PC underwent a slight thermal transition from 120°C to 125°C, during which lipid bilayers melted. Between 144°C and 148°C, cholesterol (blue line) shows a stronger endothermic peak, confirming its crystalline melting point. Polymeric relaxation and water release caused Carbopol (purple line) to heat up from 85°C to 90°C. The BC-PC phytosome complex (green line) showed decreased crystallinity and an effective BC-PC interaction at 110°C, as evidenced by a broader endothermic peak at 118°C. Most crucially, the BC-PC phytosomal gel's (yellow line) strong endothermic peak at 117.8°C, with a start temperature of 98.5°C, showed a highly ordered gel structure (Figure 8). Heat sharpens and alters peaks, indicating a homogeneous system with strong molecular interactions between the phytosomal complex and the Carbopol gel base. To confirm component transition to amorphous or molecularly dispersed, remove melting peaks in the final gel to improve formulation stability.

X-ray Diffraction (XRD) Analysis

XRD was used to investigate crystallinity and structural changes in BC-PC phytosome gels. The diffraction pattern of pure BC showed peaks in the 2θ range of 5°- 35°, indicating its high crystallinity (black line). PC (red line) and cholesterol (blue line) showed significant, sharp diffraction peaks at 2θ = 20.1°, 21.5°, and 23.2°, confirming their crystalline structures. Peak intensity and sharpness decreased significantly in the BC-PC phytosomal complex (green line) XRD pattern, indicating poorer crystallinity (Figure 9). BC phospholipid matrix and molecular interactions reduce its crystalline form to amorphous pieces. The drug's pure lattice structure is destroyed.

Additionally, the BC-PC phytosomal gel (purple line) exhibited an amorphous diffraction pattern, with no sharp peaks and a broad halo at 2θ = 18°- 25°. The phytosomal complex has correctly diffused throughout the Carbopol polymer matrix and become amorphous. Gel formulations can improve the solubility, bioavailability, and physical stability of bioactive chemicals by reducing crystalline peaks. All evidence indicates that phytosome and gel synthesis convert crystalline basic materials into a stable amorphous state (Das & Kalita, 2014).

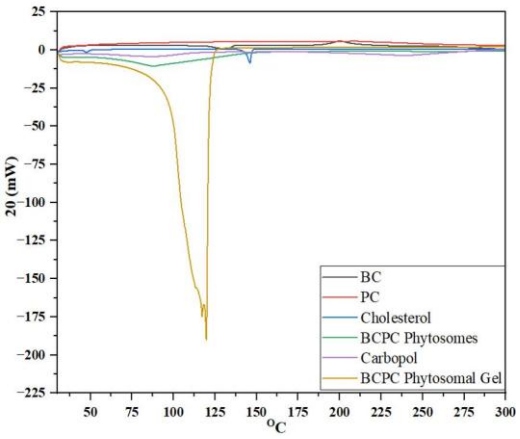


Figure 8. DSC thermogram of Pure extract and Phytosomes and phytosomal gel

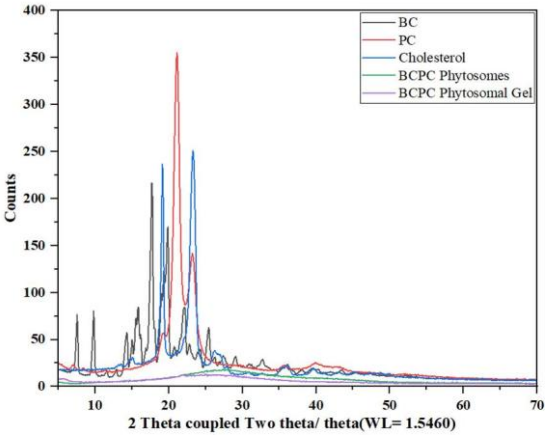


Figure 9. Powdered X-ray diffractogram of Pure extract and Phytosomes and phytosomal gel

Surface morphology using SEM& TEM

SEM of the BC-PC-phytosomes sample (Figure 10) shows that PC formed unbonded BC complexes and that the particles have no surface defects or crystalline structures. The BC-PC complex had particles of 100-200 nm, matching DLS PS homogeneity and dispersion measurements. SEM synergistically reduces PS by drying carriers and creating smaller particles than DLS. DLS calculates the hydrodynamic size of nanoparticles and liquid layers. However, SEM can be used to determine nanoparticle size (Udapurkar *et al.,* 2018). DLS measures the hydrodynamic diameter of moving particles.

In contrast, particle aggregation during measurements may increase size. Singh used SEM to identify gingerol-containing phytosomes, including uniformly sized and irregularly shaped spheres. Figure 10 C&D shows the expanded gel and optimised BCPC-phytosomes (F6), while TEM measured their shape and lamellarity. Spheres and unilamellar vesicles appeared. SEM revealed phytosome surface and three-dimensionality (Figure 10 A&B).

***In-vitro* release studies**

The prolonged release of BC-PC-phytosome and gel formulation to pure BC solution was examined in vitro. Figure 11 shows the results. The medication may slowly enter the dialysis membrane, complex release fluid, and delay release. The BC-PC combination is more soluble than hydrophobic crude BC, which may explain the notable difference in BC release patterns. After 24 hours, the free drug solution released 35.26±3.28%, whereas the F6 formulation released 80.47±0.95%, and the F6 gel formulation released 70.36±0.54%. The duration of emissions increased substantially. Drug-loaded phytosome particles rupture six hours after improved phytosomal gel delivery. Very amphiphilic surfactant PC enhanced phospholipid solubility. All nanoscale phytosomes exhibited superior surface-area selectivity compared with crude BC (Deleanu *et al.,* 2023). Phospholipids reduce hydrophobic particle and water-based surface tension, enhancing medication wettability. Lipid-encased extracts may prolong the topical release of drugs. Early or sustained release can reach therapeutic concentration. We prioritised release sequences with the highest R^2 score. The Higuchi, first-order, and zero-order models correlated best with the optimised BC-PC-phytosomal gel. Higuchi's model fit the amended formulation well after the correlation coefficient was computed. BC-PC-phytosome non-Fickian diffusion releases BC best at $n < 0.72$.

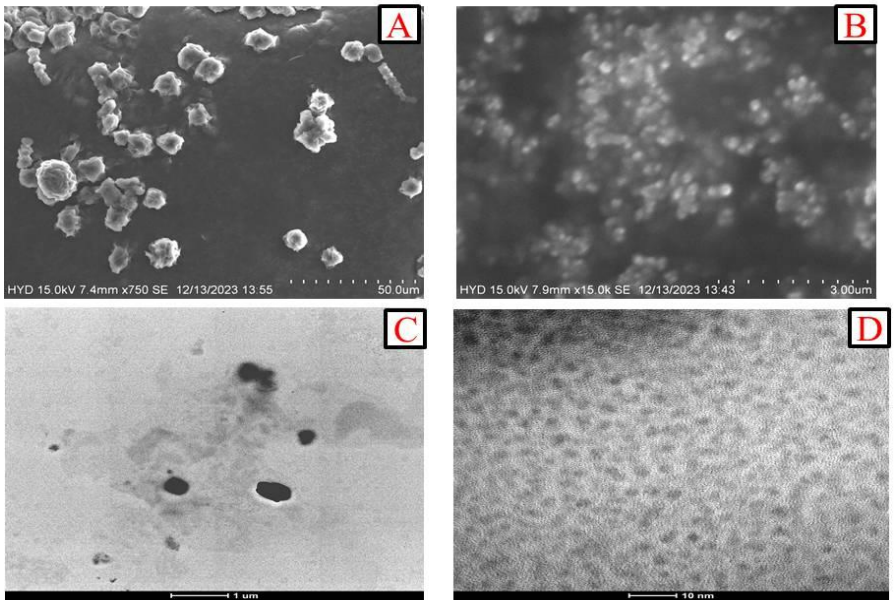


Figure 10. A& B SEM images of Phytosomes and Phytosomal gel C&D TEM images of Phytosomes and Phytosomal gel

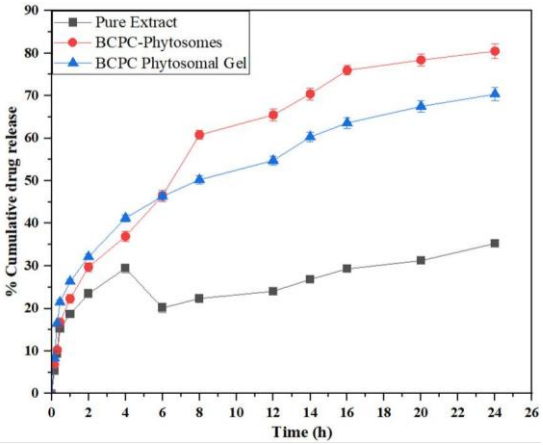


Figure 11. *In-vitro* drug release comparison studies of optimized phytosomes and phytosomal gel. Results are expressed as mean ± SD (n = 3)

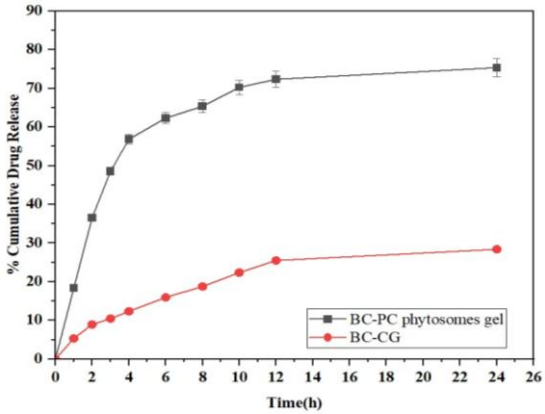


Figure 12. Percentage of cumulative drug release of the BC-PC phytosomes gel vs. conventional gel (CG) formulation. Values represent mean ± SD (n = 3)

Ex-vivo permeation study

Figure 12 and Table 5 exhibit ex vivo BC-PC phytosome gel and BC-CG skin penetration in rat abdominal skin. Formulation release was measured using a flux value graph. BC penetration (%) from BC-PC phytosomes gel and BC-CG after 24 hours: BC-PC phytosome gel (75.36±1.24) surpasses BC-CG (28.39±0.35). BC permeation flux order (mg/cm²/h ± SD): BC-PC phytosome gel (1.52±0.028) surpasses BC-CG (0.49±0.01). BC-PC phytosome gel showed the highest permeation flow, followed by BC-CG hydrogel ($p < 0.05$). At appropriate surfactant and cosurfactant concentrations, BC-PC phytosomes gel enhanced permeability and decreased the stratum corneum barrier. Due to its greater skin contact area, the BC-PC phytosomes gel demonstrated a stronger drug transport gradient. Further research focused on BC-PC phytosome gel (Recknagel *et al.,* 1989).

In - vitro Anti-inflammatory activity

BC-PC Phytosomes and phytosomal gels were better in vitro for anti-inflammatory effects. Gel formulation and BC-PC phytosomes were tested at 10-50 µg/mL concentrations. Anti-inflammatory drugs inhibit biochemical processes (Recknagel *et al.,* 1989). Protein denaturation-inhibiting BSA was used to examine anti-inflammatory effects. The approach stabilises protein structure, minimises protein aggregation, and illustrates how drugs interfere with inflammatory processes to protect BSA. The illustration shows that BC-mediated BC-PC phytosomes and gel are anti-inflammatory like gold. Sample quality was assessed at 660 nm. BC-PC phytosomes and gel were compared to the famous medicine diclofenac at 10-50 µg/mL concentrations. BC-PC phytosomes and gel showed anti-inflammatory effects of 79.86±0.30%, 82.03±0.36%, and 92.46±0.86% at 40 µg/mL compared to the reference (Figure 13). In BSA and egg albumin denaturation assays, BC-PC phytosomes decreased inflammation by 80-82%, and the phytosomal gel by 92%, comparable to or exceeding the effects of diclofenac sodium. Protein denaturation is linked to inflammation; reducing it in these studies is an early anti-inflammatory signal. Previous research indicates that in vitro medications with ≥60-70% inhibition exhibit significant anti-inflammatory effects in vivo. Clinically appropriate inhibition values apply to our improved phytosomal formulation. While translating in vitro results to clinical effectiveness is difficult, the improved BC-PC phytosomal gel's inhibition, especially compared with reference drugs, supports its anti-inflammatory properties in vivo. These findings indicate the formulation's potential in animal and translational research.

Table 5. Permeation profile and drug retention of BC in skin from BC-PC phytosomes gel and BC-CG (*n*= 3)

Formulation	Percentage of RV Permeated (% ± SD)	Permeation Flux (mg/cm²/h ± SD)	Drug Retained (mg ± SD)
BC-PC phytosomes gel	75.36±1.24	1.52±0.028	2.05±0.36
BC-CG	28.39±0.35	0.49±0.01	0.513±0.34

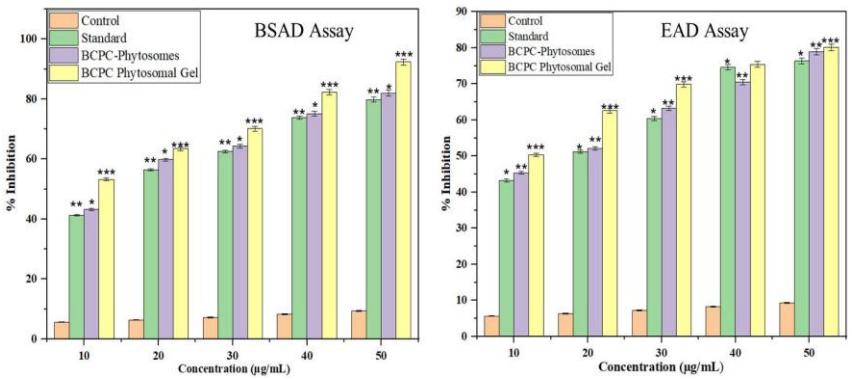


Figure 13. ***In- vitro*** **anti-inflammatory effect of formulations examined using BSAD and EAD assays at various conc. (10–50 µg/mL). Data are presented as mean ± SD (n = 3).: $p < 0.05$ (*), $p < 0.01$ (**), $p < 0.001$ (***)**

The egg albumin denaturation test heats or acidifies the protein and examines its structural and functional changes. Denaturing egg albumin shows its stability and environmental reactivity. We can comprehend protein function in living things using this information. As depicted in the image, diclofenac, BC-PC Phytosomes, and BC-PC phytosomal gel (10-50 µg/mL) were tested at various doses. A concentration of 50 µg/mL showed 76.35±0.82% anti-inflammatory effect as a reference, and 80.12±0.94% for BC-PC phytosomal gel ([82]). Groups were compared using GraphPad Prism's one-way ANOVA with Tukey's post hoc test. The updated picture legend clearly defines significance markers and aligns with established p-value thresholds: $p < 0.05$ (*), $p < 0.01$ (**), and $p < 0.001$ (***).

This study successfully manufactures and evaluates an anti-inflammatory BC-PC phytosomal gel; it has drawbacks. The study did not compare phytochemical or functional assessments with a certified, standardised broccoli extract to assess equivalence and repeatability. In-vitro protein denaturation assays were used to examine the anti-inflammatory effect, which may show biological potential but cannot fully anticipate the complicated multi-step inflammatory pathways encountered in in-vivo or clinical situations. The phytochemical characterisation focused on phenolic, flavonoid, and tannin content, neglecting bioactive compounds such as sulforaphane, quercetin derivatives, and glucosinolates that could affect therapeutic benefits. The study lacks pharmacokinetic, toxicological, and long-term stability data needed for translational or clinical usage. Standardised extract comparisons, in vivo efficacy models, phytochemical profiling, and safety and stability tests are needed to determine the medicinal usefulness of the phytosomal gel.

Limitations: This study possesses some shortcomings that warrant acknowledgement. The phytochemical characterisation and partition analysis were conducted using UV-Visible spectrophotometry, which provides a general assessment of extract constituents but fails to identify specific bioactive compounds; more sophisticated analytical methods, such as HPLC or LC-MS, would yield greater specificity. Secondly, the study employed ex vivoex vivo Wistar rat skin to evaluate permeability, which may not accurately reflect human skin physiology, thereby limiting generalisability to clinical scenarios. Third, while the Box–Behnken design facilitated effective optimisation of formulation parameters, the model was constrained by a limited experimental range and may not adequately account for variability across different extract batches or in large-scale manufacturing. Furthermore, the anti-inflammatory experiments were performed in vitro and may not accurately represent the intricate biological responses observed in vivo. This study did not assess long-term stability, the potential for skin irritation, or therapeutic efficacy in animal models, all of which are critical for translational use. Subsequent research must address these deficiencies before endorsing clinical application.

Conclusions

BC-PC-loaded phytosomes were successfully made via thin lipid film hydration. In a BBD design, PS, EE, and % CDR were compared to three independent variables. Formulation F6, with the lowest PS (127.49±5.64 nm) and highest EE (89.12±1.03%) for BC-PC phytosomes, was selected. The thermogel formulation was then

modified using the enhanced phytosome formulation and tested for skin compatibility. FTIR, DSC, XRD, and partition coefficient analyses were used to evaluate phytosome and phytosomal gel formulations. The gel with lower logP values showed a nanoscale vesicular structure with better solubility than the reference gel. Thus, BC-PC-loaded phytosomal gel may be clinically effective for RA treatment as nanosized vesicles. The BC-PC phytosomal gel has promising physicochemical properties and in vitro anti-inflammatory activity, but further studies are needed to confirm its translational and therapeutic effects. To ensure the phytosomal system's physical and chemical integrity during storage, future studies must include long-term stability tests. To determine topical safety, in vitro safety tests must include cytotoxicity assays on relevant dermal cell lines and skin irritation/sensitisation studies. To confirm the enhanced permeability and anti-inflammatory effects in vitro, in vivo pharmacokinetic and therapeutic studies are needed. The BC-PC phytosomal gel must meet regulatory standards, formulation scale-up, and batch consistency to advance to preclinical and clinical development.

Funding

The authors received no specific financial support for the research, authorship, and/or publication of this article.

Author Contributions

Conceptualization: S.C.; Methodology: S.C.; Investigation: S.F.; Data curation: S.C.; Writing - original draft: S.C.; Writing - review & editing: S.C., S.S.; Supervision: S.S. All authors have read and agreed to the published version of the manuscript.

Ethics Statement

The study was approved by the Institutional Animal Ethics Committee (IAEC) of Jeeva Life Sciences, Uppal, Hyderabad, India (Approval No. CPCSEA/IAEC/JLS/08/02/25/002). All animal experiments were conducted in accordance with relevant ethical guidelines and regulations.

Declaration of Generative AI Use

The authors declare that no Generative AI tools were used in the preparation of this manuscript.

Conflict of Interest

The authors declare that they have no conflicts of interest related to this work.

Data Availability Statement

No new data were generated or analyzed in support of this research.

Acknowledgement

The authors have no acknowledgements to declare.

References

Lumley, M. A., Anderson, T., Ankawi, B., Goldman, G., Perri, L. M., Bianco, J. A., & Keefe, F. J. (2018). The working alliance and clinician-assisted emotional disclosure for rheumatoid arthritis. *Journal of Psychosomatic Research, 104*, 9-15. https://doi.org/10.1016/j.jpsychores.2017.11.004

Yao, Y., Cai, X., Yu, H., Xu, Q., Li, X., Yang, Y., Meng, X., Huang, C., & Li, J. (2019). PSTPIP2 attenuates joint damage and suppresses inflammation in adjuvant-induced arthritis. *European Journal of Pharmacology, 859*, 172558. https://doi.org/10.1016/j.ejphar.2019.172558

Das, T., Prakash, V. M., & Math, P. K. (2019). Injectable in situ gel of methotrexate for rheumatoid arthritis: Development, in vitro and in vivo evaluation. *Journal of Applied Pharmaceutical Science, 9*(5), 40-48. https://doi.org/10.7324/JAPS.2019.90505

Wang, W., Zhou, H., & Liu, L. (2020). The role of Chinese herbal medicine in the management of adverse drug reactions of leflunomide in treating rheumatoid arthritis. *Phytomedicine, 68*, 153136. https://doi.org/10.1016/j.phymed.2019.153136

Vona, R., Gambardella, L., Cittadini, C., Straface, E., & Pietraforte, D. (2019). Biomarkers of oxidative stress in metabolic syndrome and associated diseases. *Oxidative Medicine and Cellular Longevity, 2019*(1), 8267234. https://doi.org/10.1155/2019/8267234

Maloberti, A., Vallerio, P., Triglione, N., Occhi, L., Panzeri, F., Bassi, I., Pansera, F., Piccinelli, E., Peretti, A., Garatti, L., & Palazzini, M. (2019). Vascular aging and disease of the large vessels: Role of inflammation. *High Blood Pressure & Cardiovascular Prevention, 26*(3), 175-182. https://doi.org/10.1007/s40292-019-00318-4

Neha, K., Haider, M. R., Pathak, A., & Yar, M. S. (2019). Medicinal prospects of antioxidants: A review. *European Journal of Medicinal Chemistry, 178*, 687-704. https://doi.org/10.1016/j.ejmech.2019.06.010

Azzi, A. (2017). Antioxidants: Wonder drugs or quackery? *BioFactors, 43*(6), 785-788. https://doi.org/10.1002/biof.1388

Forman, H. J., & Zhang, H. (2021). Targeting oxidative stress in disease: Promise and limitations of antioxidant therapy. *Nature Reviews Drug Discovery, 20*(9), 689-709. https://doi.org/10.1038/s41573-021-00233-1

Savjani, K. T., Gajjar, A. K., & Savjani, J. K. (2012). Drug solubility: Importance and enhancement techniques. *ISRN Pharmaceutics, 2012*, Article 195727. https://doi.org/10.5402/2012/195727

Gupta, S., Kesarla, R., & Omri, A. (2013). Formulation strategies to improve the bioavailability of poorly absorbed drugs with special emphasis on self-emulsifying systems. *ISRN Pharmaceutics, 2013*, Article 848043. https://doi.org/10.1155/2013/848043

Rajan, R., Jose, S., Mukund, V. B., & Vasudevan, D. T. (2011). Transferosomes: A vesicular transdermal delivery system for enhanced drug permeation. *Journal of Advanced Pharmaceutical Technology & Research, 2*(3), 138-143. https://doi.org/10.4103/2231-4040.85524

Mishra, N., Yadav, N. P., Meher, J. G., & Sinha, P. (2012). Phyto-vesicles: Conduit between conventional and novel drug delivery system. *Asian Pacific Journal of Tropical Biomedicine, 2*(3), S1728-S1734. https://doi.org/10.1016/S2221-1691(12)60485-7

Saraf, S. (2010). Applications of novel drug delivery system for herbal formulations. *Fitoterapia, 81*(7), 680-689. https://doi.org/10.1016/j.fitote.2010.05.001

Recio, M. C., Andújar, I., & Ríos, J. L. (2012). Anti-inflammatory agents from plants: Progress and potential. *Current Medicinal Chemistry, 19*(14), 2088-2103. https://doi.org/10.2174/092986712800229069

Eberhardt, M. V., Lee, C. Y., & Liu, R. H. (2000). Antioxidant activity of fresh apples. *Nature, 405*, 903-904. https://doi.org/10.1038/35016151

Spagnuolo, C., Russo, M., Bilotto, S., Tedesco, I., Laratta, B., & Russo, G. L. (2012). Dietary polyphenols in cancer prevention: The example of the flavonoid quercetin in leukemia. *Annals of the New York Academy of Sciences, 1259*(1), 95-103. https://doi.org/10.1111/j.1749-6632.2012.06599.x

Andriantsitohaina, R., Auger, C., Chataigneau, T., Étienne-Selloum, N., Li, H., Martínez, M. C., Schini-Kerth, V. B., & Laher, I. (2012). Molecular mechanisms of the cardiovascular protective effects of polyphenols. *British Journal of Nutrition, 108*(9), 1532-1549. https://doi.org/10.1017/S0007114512003406

Vauzour, D., Rodriguez-Mateos, A., Corona, G., Oruna-Concha, M. J., & Spencer, J. P. (2010). Polyphenols and human health: Prevention of disease and mechanisms of action. *Nutrients, 2*(11), 1106-1131. https://doi.org/10.3390/nu2111106

Ansari, M. T., Sami, F., Khairudiin, F. A., Atan, M. Z., bin Tengku Mohamad, T. A., Majeed, S., & Ali, S. (2018). Applications of zinc nanoparticles in medical and healthcare fields. *Current Nanomedicine, 8*(3), 225-233. https://doi.org/10.2174/2405461503666180709100110

Majeed, S., bin Abdullah, M. S., Nanda, A., & Ansari, M. T. (2016). In vitro study of the antibacterial and anticancer activities of silver nanoparticles synthesized from *Penicillium brevicompactum* (MTCC-1999). *Journal of Taibah University for Science, 10*(4), 614-620. https://doi.org/10.1016/j.jtusci.2016.02.010

Ansari, M. T., Risheshwar, P., & Ali, S. (2017). Effect of hydroxy acids and organic bases on complexation efficiency of aceclofenac beta cyclodextrin inclusion complex. *European Journal of Biomedical and Pharmaceutical Sciences, 4*(5), 586-589.

Nayak, A. K., Mazumder, S., Ara, T. J., Ansari, M. T., & Hasnain, M. S. (2019). Calcium fluoride-based dental nanocomposites. In A. M. Asiri, Inamuddin, & A. Mohammad (Eds.), *Applications of nanocomposite materials in dentistry* (pp. 27-45). Elsevier. https://doi.org/10.1016/B978-0-12-813742-0.00002-X

Miraj, S. (2016). Broccoli (*Brassica oleracea* var. *italica*): Potential candidate in the health management. *Der Pharmacia Lettre, 8*(14), 61-65.

Owis, A. I. (2015). Broccoli: The green beauty: A review. *Journal of Pharmaceutical Sciences and Research, 7*(9), 696-703.

Mahn, A., & Reyes, A. (2012). An overview of health-promoting compounds of broccoli (*Brassica oleracea* var. *italica*) and the effect of processing. *Food Science and Technology International, 18*(6), 503-514. https://doi.org/10.1177/1082013211433073

Deep, P., Singh, A. K., Ansari, M. T., & Raghav, P. (2013). Pharmacological potentials of *Ficus racemosa*: A review. *International Journal of Pharmaceutical Sciences Review and Research, 22*(1), 29-34.

Badgujar, V. B., Ansari, M. T., Abdullah, M. S., & Badgujar, S. V. (2015). Homoharringtonine: A nascent phytochemical for cancer treatment (A review). *World Journal of Pharmacy and Pharmaceutical Sciences, 4*(12), 1380-1391.

Prabowo, S. (2019). Broccoli extract (*Brassica oleracea*) decreases periarticular malondialdehyde level and disease activity score in rats (*Rattus norvegicus*) with adjuvant arthritis. *IOP Conference Series: Earth and Environmental Science, 217*(1), Article 012046. https://doi.org/10.1088/1755-1315/217/1/012046

Khan, J., Alexander, A., Saraf, S., & Saraf, S. (2013). Recent advances and future prospects of phyto-phospholipid complexation technique for improving pharmacokinetic profile of plant actives. *Journal of Controlled Release, 168*(1), 50-60. https://doi.org/10.1016/j.jconrel.2013.02.025

Naz, Z., & Ahmad, F. J. (2015). Curcumin-loaded colloidal carrier system: Formulation optimization, mechanistic insight, ex vivo and in vivo evaluation. *International Journal of Nanomedicine, 10*, 4293-4307. https://doi.org/10.2147/IJN.S82788

Rapalli, V. K., Kaul, V., Gorantla, S., Waghule, T., Dubey, S. K., Pandey, M. M., & Singhvi, G. (2020). UV spectrophotometric method for characterization of curcumin loaded nanostructured lipid nanocarriers in simulated conditions: Method development, in-vitro and ex-vivo applications in topical delivery. *Spectrochimica Acta Part A: Molecular and Biomolecular Spectroscopy, 224*, 117392. https://doi.org/10.1016/j.saa.2019.117392

Golwala, P., Rathod, S., Patil, R., Joshi, A., Ray, D., Aswal, V. K., Bahadur, P., & Tiwari, S. (2020). Effect of cosurfactant addition on phase behavior and microstructure of a water dilutable microemulsion. *Colloids and Surfaces B: Biointerfaces, 186*, Article 110736. https://doi.org/10.1016/j.colsurfb.2019.110736

Zhu, L., Zhang, Z., Xia, N., Zhang, W., Wei, Y., Huang, J., Ren, Z., Meng, F., & Yang, L. (2020). Anti-arthritic activity of ferulic acid in complete Freund's adjuvant (CFA)-induced arthritis in rats: JAK2 inhibition. *Inflammopharmacology, 28*(2), 463-473. https://doi.org/10.1007/s10787-019-00642-0

Haque, M., Singh, A. K., Ouseph, M. M., & Ahmed, S. (2021). Regulation of synovial inflammation and tissue destruction by guanylate binding protein 5 in synovial fibroblasts from patients with rheumatoid arthritis and rats with adjuvant-induced arthritis.

Arthritis & Rheumatology, 73(6), 943-954. https://doi.org/10.1002/art.41611

Lubberts, E., & van den Berg, W. B. (2003). Cytokines in the pathogenesis of rheumatoid arthritis and collagen-induced arthritis. In P. Santamaria (Ed.), *Cytokines and chemokines in autoimmune disease* (Advances in Experimental Medicine and Biology, Vol. 520, pp. 194-202). Springer. https://doi.org/10.1007/978-1-4615-0171-8_11

Feldmann, M., Brennan, F. M., Williams, R. O., Woody, J. N., & Maini, R. N. (2004). The transfer of a laboratory based hypothesis to a clinically useful therapy: The development of anti-TNF therapy of rheumatoid arthritis. *Best Practice & Research Clinical Rheumatology, 18*(1), 59-80. https://doi.org/10.1016/j.berh.2003.09.010

Rahman, M. A., Kamal, M., & Hussain, A. (2015). Phytochemical and analytical evaluation of Kachnal (*Bauhinia racemosa* Lam.) bark. *Current Traditional Medicine, 1*(2), 136-144. https://doi.org/10.2174/2215083801666150709164815

Telange, D. R., Patil, A. T., Pethe, A. M., Fegade, H., Anand, S., & Dave, V. S. (2017). Formulation and characterization of an apigenin-phospholipid phytosome (APLC) for improved solubility, in vivo bioavailability, and antioxidant potential. *European Journal of Pharmaceutical Sciences, 108*, 36-49. https://doi.org/10.1016/j.ejps.2016.12.009

Mane, V., Killedar, S., More, H., Nadaf, S., Salunkhe, S., & Tare, H. (2024). Novel phytosomal formulation of *Emblica officinalis* extracts with its in vivo nootropic potential in rats: Optimization and development by Box-Behnken design. *Journal of Chemistry, 2024*(1), 6644815. https://doi.org/10.1155/2024/6644815

Rarokar, N., C, R., Gurav, S., & Khedekar, P. (2021). Meloxicam encapsulated nanostructured colloidal self-assembly for evaluating antitumor and anti-inflammatory efficacy in 3D printed scaffolds. *Journal of Biomedical Materials Research Part A, 109*(8), 1441-1456. https://doi.org/10.1002/jbm.a.37135

Tetyczka, C., Hodzic, A., Kriechbaum, M., Juraić, K., Spirk, C., Hartl, S., Pritz, E., Leitinger, G., & Roblegg, E. (2019). Comprehensive characterization of nanostructured lipid carriers using laboratory and synchrotron X-ray scattering and diffraction. *European Journal of Pharmaceutics and Biopharmaceutics, 139*, 153-160. https://doi.org/10.1016/j.ejpb.2019.03.017

Maiti, K., Mukherjee, K., Murugan, V., Saha, B. P., & Mukherjee, P. K. (2009). Exploring the effect of hesperetin-HSPC complex: A novel drug delivery system on the in vitro release, therapeutic efficacy and pharmacokinetics. *AAPS PharmSciTech, 10*(3), 943-950. https://doi.org/10.1208/s12249-009-9282-6

Kiran, P. M., Raju, A. V., & Rao, B. G. (2012). Investigation of hepatoprotective activity of *Cyathea gigantea* (Wall. ex Hook.) leaves against paracetamol-induced hepatotoxicity in rats. *Asian Pacific Journal of Tropical Biomedicine, 2*(5), 352-356. https://doi.org/10.1016/S2221-1691(12)60055-0

Danowski, T. S., Stephan, T., Nolan, S., Ahmad, U., Wingert, J. P., Jr., Bowman, D. H., Sunder, J. H., & Fisher, E. R. (1976). Thyroid hormone-like effects without thyrotoxicosis during one year's therapy with Na-DT3 for hypercholesterolemia. *Clinical Pharmacology & Therapeutics, 19*(2), 196-205. https://doi.org/10.1002/cpt1976192196

Ng, R. H., Kiechle, F. L., Whelan, P. V., Graham, J., Jackson, B., McGill, C., Greenfield, K., Igo, S., Reynolds, L., Shepherd, S., & Peterson, V. (1993). Multicenter evaluation of a urine analyzer. *Laboratory Medicine, 24*(12), 783-789. https://doi.org/10.1093/labmed/24.12.783

Ellman, G. L. (1959). Tissue sulfhydryl groups. *Archives of Biochemistry and Biophysics, 82*(1), 70-77. https://doi.org/10.1016/0003-9861(59)90090-6

Marklund, S., & Marklund, G. (1974). Involvement of the superoxide anion radical in the autoxidation of pyrogallol and a convenient assay for superoxide dismutase. *European Journal of Biochemistry, 47*(3), 469-474. https://doi.org/10.1111/j.1432-1033.1974.tb03714.x

Stocks, J., & Dormandy, T. L. (1971). The autoxidation of human red cell lipids induced by hydrogen peroxide. *British Journal of Haematology, 20*(1), 95-111. https://doi.org/10.1111/j.1365-2141.1971.tb00790.x

Beers, R. F., Jr., & Sizer, I. W. (1952). A spectrophotometric method for measuring the breakdown of hydrogen peroxide by catalase. *Journal of Biological Chemistry, 195*(1), 133-140. https://doi.org/10.1016/S0021-9258(19)50881-X

Abdullah, Khan, M. A., Ahmad, W., Ahmad, M., & Nisar, M. (2017). Hepatoprotective effect of the solvent extracts of *Viola canescens* Wall. ex Roxb. against CCl4 induced toxicity through antioxidant and membrane stabilizing activity. *BMC Complementary and Alternative Medicine, 17*(1), 10. https://doi.org/10.1186/s12906-016-1537-7

Dhore, P. W., Dave, V. S., Saoji, S. D., Bobde, Y. S., Mack, C., & Raut, N. A. (2017). Enhancement of the aqueous solubility and permeability of a poorly water-soluble drug ritonavir via lyophilized milk-based solid dispersions. *Pharmaceutical Development and Technology, 22*(1), 90-102. https://doi.org/10.1080/10837450.2016.1193193

Duan, K., Yuan, Z., Guo, W., Meng, Y., Cui, Y., Kong, D., Zhang, L., & Wang, N. (2011). LC-MS/MS determination and pharmacokinetic study of five flavone components after solvent extraction/acid hydrolysis in rat plasma after oral administration of *Verbena officinalis* L. extract. *Journal of Ethnopharmacology, 135*(2), 201-208. https://doi.org/10.1016/j.jep.2011.01.002

Gurav, R., Hwang, S., Bhatia, S. K., Kshirsagar, A. D., Mandal, S., & Yang, Y. H. (2025). Exopolysaccharide production using pinewood hydrolysate as a substrate for psychrotrophic bacterium isolated from Svalbard glacier soil. *Biomass Conversion and Biorefinery, 15*(2), 2263-2273. https://doi.org/10.1007/s13399-023-05039-2

Nair, A. B., & Jacob, S. (2016). A simple practice guide for dose conversion between animals and human. *Journal of Basic and Clinical Pharmacy, 7*(2), 27-31. https://doi.org/10.4103/0976-0105.177703

Chen, T., Li, L. P., Lu, X. Y., Jiang, H. D., & Zeng, S. (2007). Absorption and excretion of luteolin and apigenin in rats after oral administration of *Chrysanthemum morifolium* extract. *Journal of Agricultural and Food Chemistry, 55*(2), 273–277. https://doi.org/10.1021/jf062088r

Sajid, M., Khan, M. R., Shah, N. A., Shah, S. A., Ismail, H., Younis, T., & Zahra, Z. (2016). Phytochemical, antioxidant and hepatoprotective effects of *Alnus nitida* bark in carbon tetrachloride challenged Sprague Dawley rats. *BMC Complementary and Alternative Medicine, 16*(1), Article 268. https://doi.org/10.1186/s12906-016-1245-3

Lu, M., Qiu, Q., Luo, X., Liu, X., Sun, J., Wang, C., Lin, X., Deng, Y., & Song, Y. (2019). Phyto-phospholipid complexes (phytosomes): A novel strategy to improve the bioavailability of active constituents. *Asian Journal of Pharmaceutical Sciences, 14*(3), 265-274. https://doi.org/10.1016/j.ajps.2018.05.011

Poonia, N., Lather, V., Kaur, B., Kirthanashri, S. V., & Pandita, D. (2020). Optimization and development of methotrexate- and resveratrol-loaded nanoemulsion formulation using Box-Behnken design for rheumatoid arthritis. *Assay and Drug Development Technologies, 18*(8), 356-368. https://doi.org/10.1089/adt.2020.989

Azeez, N. A., Deepa, V. S., & Sivapriya, V. (2018). Phytosomes: Emergent promising nano vesicular drug delivery system for targeted tumor therapy. *Advances in Natural Sciences: Nanoscience and Nanotechnology, 9*(3), 033001. https://doi.org/10.1088/2043-6254/aadc50

Sharma, S., Shukla, P., Misra, A., & Mishra, P. R. (2014). Interfacial and colloidal properties of emulsified systems: Pharmaceutical and biological perspective. In H. Ohshima & K. Makino (Eds.), *Colloid and interface science in pharmaceutical research and development* (pp. 149-172). Elsevier. https://doi.org/10.1016/B978-0-444-62614-1.00008-9

United States Pharmacopeial Convention [USP]. (1989). *The United States Pharmacopeia: USP 22* (22nd rev.). United States Pharmacopeial Convention.

Saoji, S. D., Raut, N. A., Dhore, P. W., Borkar, C. D., Popielarczyk, M., & Dave, V. S. (2016). Preparation and evaluation of phospholipid-based complex of standardized centella extract (SCE) for the enhanced delivery of phytoconstituents. *The AAPS Journal, 18*(1), 102-114. https://doi.org/10.1208/s12248-015-9837-2

Ahmed, O. A., & Badr-Eldin, S. M. (2019). Development of an optimized avanafil-loaded invasomal transdermal film: Ex vivo skin permeation and in vivo evaluation. *International Journal of Pharmaceutics, 570*, 118657. https://doi.org/10.1016/j.ijpharm.2019.118657

Zhang, Y. R., Lin, R., Li, H. J., He, W. L., Du, J. Z., & Wang, J. (2019). Strategies to improve tumor penetration of nanomedicines through nanoparticle design. *Wiley Interdisciplinary Reviews: Nanomedicine and Nanobiotechnology, 11*(1), e1519. https://doi.org/10.1002/wnan.1519

Metkari, V., Shah, R., Salunkhe, N., & Gurav, S. (2023). QbD approach for the design, optimization, development, and characterization of naringenin-loaded phytosomes to enhance solubility and oral bioavailability. *Journal of Pharmaceutical Innovation, 18*(4), 2083-2097. https://doi.org/10.1007/s12247-023-09775-w

Dubey, V., Mishra, D., Dutta, T., Nahar, M., Saraf, D. K., & Jain, N. K. (2007). Dermal and transdermal delivery of an anti-psoriatic agent via ethanolic liposomes. *Journal of Controlled Release, 123*(2), 148-154. https://doi.org/10.1016/j.jconrel.2007.08.005

Mehanna, M. M., El-Kader, N. A., & Samaha, M. W. (2017). Liposomes as potential carriers for ketorolac ophthalmic delivery: Formulation and stability issues. *Brazilian Journal of Pharmaceutical Sciences, 53*(2), e16127. https://doi.org/10.1590/s2175-97902017000216127

Rathee, S., & Kamboj, A. (2018). Optimization and development of antidiabetic phytosomes by the Box-Behnken design. *Journal of Liposome Research, 28*(2), 161-172. https://doi.org/10.1080/08982104.2017.1311913

Islam, N., Irfan, M., Hussain, T., Mushtaq, M., Khan, I. U., Yousaf, A. M., Ghori, M. U., & Shahzad, Y. (2022). Piperine phytosomes for bioavailability enhancement of domperidone. *Journal of Liposome Research, 32*(2), 172-180. https://doi.org/10.1080/08982104.2021.1918153

Fathi, F., Kouchaksaraee, R. M., Ebrahimi, S. N., Costa, A. S., Souto, E. B., Prior, J. A., Oliveira, M. B., & Alves, R. C. (2023). Enhanced-release of phenolic-enriched grape seed antioxidants through innovative cholesterol doped phytosomes. *Sustainable Materials and Technologies, 37*, e00673. https://doi.org/10.1016/j.susmat.2023.e00673

Orlandi, G., Bari, E., Catenacci, L., Sorrenti, M., Segale, L., Faragò, S., Sorlini, M., Arciola, C. R., Torre, M. L., & Perteghella, S. (2020). Polyphenols-loaded sericin self-assembling nanoparticles: A slow-release for regeneration by tissue-resident mesenchymal stem/stromal cells. *Pharmaceutics, 12*(4), 381. https://doi.org/10.3390/pharmaceutics12040381

Govindaram, L. K., Al Bratty, M., Alhazmi, H. A., Kandasamy, R., Thangavel, N., Ibrahim, A. M., Mariya, G. A., & Kumar, P. (2022). Formulation, biopharmaceutical evaluation and in-vitro screening of polyherbal phytosomes for breast cancer therapy. *Drug Development and Industrial Pharmacy, 48*(10), 552-565. https://doi.org/10.1080/03639045.2022.2138911

Corrie, L., Gundaram, R., & Kukatil, L. (2021). Formulation and evaluation of *Cassia tora* phytosomal gel using central composite design. *Recent Innovations in Chemical Engineering, 14*(4), 347-357. https://doi.org/10.2174/2405520414666210525094503

Das, M. K., & Kalita, B. (2014). Design and evaluation of phyto-phospholipid complexes (phytosomes) of rutin for transdermal application. *Journal of Applied Pharmaceutical Science, 4*(10), 51-57. https://doi.org/10.7324/JAPS.2014.401010

Udapurkar, P. P., Bhusnure, O. G., & Kamble, S. R. (2018). Diosmin phytosomes: Development, optimization and physicochemical characterization. *Indian Journal of Pharmaceutical Education and Research, 52*(4), S29-S36. https://doi.org/10.5530/ijper.52.4s.73

Deleanu, M., Toma, L., Sanda, G. M., Barbălată, T., Niculescu, L. Ş., Sima, A. V., Deleanu, C., Săcărescu, L., Suciu, A., Alexandru, G., & Crișan, I. (2023). Formulation of phytosomes with extracts of ginger rhizomes and rosehips with improved bioavailability, antioxidant and anti-inflammatory effects in vivo. *Pharmaceutics, 15*(4), 1066. https://doi.org/10.3390/pharmaceutics15041066

Recknagel, R. O., Glende, E. A., Jr., Dolak, J. A., & Waller, R. L. (1989). Mechanisms of carbon tetrachloride toxicity. *Pharmacology & Therapeutics, 43*(1), 139-154. https://doi.org/10.1016/0163-7258(89)90050-8